# Potential of biocompatible polymeric ultra-thin films, nanosheets, as topical and transdermal drug delivery devices

Tomomi Hatanaka[a,b,*], Takanori Saito[a], Takaaki Fukushima[a], Hiroaki Todo[a], Kenji Sugibayashi[a], Soichi Umehara[a], Tomoharu Takeuchi[a], Yosuke Okamura[c]

[a]Faculty of Pharmacy and Pharmaceutical Sciences, Josai University, 1-1 Keyakidai, Sakado, Saitama 350-0295, Japan

[b]Tokai University School of Medicine, 143 Shimokasuya, Isehara, Kanagawa 259-1193, Japan

[c]Tokai University School of Engineering, 4-1-1 Kitakaname, Hiratsuka, Kanagawa 259-1292, Japan

[*]Corresponding author.

E-mail address: tmmhtnk@josai.ac.jp (T. Hatanaka)

## ABSTRACT

The aim of the present study was to assess the potential of biocompatible polymeric nanosheets as topical and transdermal drug-delivery devices. Nanosheets are two-dimensional nanostructures with a thickness in the nanometer order, and their extremely large aspect ratios result in unique properties, including high transparency, flexibility, and adhesiveness. Nanosheet formulations containing betamethasone valerate (BV) as a model drug and consisting of poly (L-lactic acid) or poly (lactic-co-glycolic) acid were fabricated through a spin-coating-assisted layer-by-layer method using a water-soluble sacrificial membrane. The fabricated formulations could incorporate and release higher amounts of BV compared with a commercial ointment, and the amounts could be controlled by the polymers used, the amount of BV added, and the use of controlled-release membranes. The presence of BV had a minimal effect on thickness, transparency, adhesiveness, and moisture permeability of nanosheets, permitting their application to any area of skin for a long period of time. Therefore, this biocompatible polymeric nanosheet formulation represents a novel and promising topical and transdermal drug delivery device, which has potential to deliver drugs regardless of the area of skin.



**Keywords:** Nanosheet, Poly (L-lactic acid), Poly (lactic-co-glycolic) acid, Topical drug delivery, Transdermal drug delivery, Betamethasone valerate

## 1. Introduction

Nanotechnology, the engineering and manufacturing of materials at the atomic and molecular scale, has had an impact on pharmaceutical technology (Farokhzad and Langer**,** 2009). Since nanoparticle formulations appeared in the 1970s (Gregoriadis, 1978; Couvreur et al., 1977), various nanostructures, such as dendrimers (Cheng et al., 2008), nanohydrogels (Dalwadi and Patel, 2015), nanoemulsions (Sarker, 2005), nanoliposomes (Gregoriadis, 1978), and nanofibers (Hu et al., 2014), have been utilized for the development of new dosing formulations for pharmaceuticals. These nanostructures provide certain functions to the dosing mechanism, including the improved dissolution of slightly soluble drugs, the enhanced transport of impermeable drugs across the epithelial and endothelial barriers, and cell- or tissue-specific targeted delivery of drugs. Nanotechnology continues to further advance drug-delivery strategies.

Ultra-thin films, often called nanosheets, are two-dimensional nanostructures with a thickness in the nanometer order (Kado et al., 2005; Cheng et al., 2009). Their extremely large aspect ratios, greater than $10^9$ depending on surface area, result in markedly different physical, chemical, and electronic characteristics from their bulk state. Therefore, nanosheets have been developed for a variety of applications, including separation membranes, light-emitting devices, friction-reducing coatings, chemical/mechanical sensors, and chemical/biological reactors (Osada and Sasaki, 2012; Liu et al., 2016). One of the earliest types of nanosheet used for medical applications was graphene, a single layer of carbon atoms arranged in a hexagonal lattice, which is capable of free existence (Goenka et al., 2014). The high drug-loading capacity due to two-dimensional structure and delocalized surface π electrons of graphene is an advantage for the delivery of chemotherapeutics and other drugs. Unfortunately, bioincompatibility and cytotoxicity induced by graphene

nanomaterials have often been reported (Liao et al., 2018). We previously fabricated free-standing polymeric nanosheets composed of biocompatible and biodegradable polymers such as chitosan and poly (L-lactic acid) (PLA) for use as materials for pharmaceuticals (Okamura et al., 2009; Komachi et al., 2017). The nanosheets, which are completely different from electrospun mats, could be used as adhesive-free alternatives to surgical sutures, wound healing dressings and postsurgical adhesion prevention sheets (Okamura et al., 2009; Okamura et al., 2013). Further medical application, such as drug delivery devices, is expected because of their high transparency, flexibility, and adhesiveness. On the other hand, there is a concern that ultra-thin nanosheets cannot incorporate and release drugs at therapeutic levels.

Transdermal therapeutic systems are mechanisms of dosing that deliver effective amounts of drugs to the systemic circulation via the skin (Tanner and Marks, 2008; Cevc et al., 1996). Compared with oral dosage forms, they have great therapeutic advantages; overcoming the first-pass metabolism of drugs, sustained systemic drug delivery, improved patient compliance, and reduced side effects. Skin has also been the administration site of therapeutic agents for skin diseases and disorders since ancient times (Chang et al., 2013). A variety of topical and transdermal drug-delivery systems now exist.

These systems are roughly classified as solid formulations, e.g. dermal patches, tapes, plasters, and cataplasms, semi-solid formulations, e.g. ointments, creams, and gels, and liquid formulations, e.g. emulsions and lotions (Sugibayashi, 2017). When a solid formulation is applied onto the patient's skin, the formulation adheres to an area of skin by an adhesive, and drug molecules diffuse from the reservoir and/or adhesive layer to the skin surface at a certain rate controlled by a semipermeable membrane and/or adhesive layer. Hence, the drug delivery is reliable throughout the therapeutic period; however, the application of this formulation is limited to relatively flat skin

surface. Reapplication of these formulations often damages the stratum corneum and causes dermatitis accompanied with symptoms such as erythema, itching, and edema (Ale et al., 2009; Yataba et al., 2016). Conversely, semi-solid and liquid formulations can be applied to any location, including the skin overlaying joints, such as the elbow and knee. However, they are weak in the presence of friction and can be easily removed when the skin is rubbed (Tang et al., 2010). If polymeric nanosheets can incorporate and release therapeutically required quantities of any drug, this will aid the development of novel topical and transdermal drug delivery devices that are applicable to any part of the skin without the need for adhesives and backing.

The present study was conducted to assess the potential of biocompatible polymeric nanosheets as topical and transdermal drug delivery devices. The nanosheets were fabricated through a spin-coating-assisted layer-by-layer method using a water-soluble sacrificial membrane (Okamura et al., 2009; Fujie et al., 2007). PLA and poly (lactic-co-glycolic) acid (PLGA) were used as the building blocks of nanosheets, and poly (vinyl alcohol) (PVA) was used as a sacrificial layer. A steroidal anti-inflammatory drug, betamethasone valerate (BV) included in the topical ointments, creams, and lotions for the treatment of various skin diseases and irritation (Drugs.com, 2018), was chosen as a model drug. The morphology, drug-loading capacity, adhesiveness, and moisture permeability of various nanosheets were evaluated. BV release from nanosheet formulations was measured under various conditions to clarify the effects of BV concentration, molecular weight of PLA, LA:GA molecular ratio, and rate-controlling membrane on release behavior. BV release from formulations and BV concentration in pig skin after topical application of the formulations were compared between nanosheet formulations and a commercial ointment product.

## 2. Materials and methods

*2.1. Materials, animals, and subjects*

PLA (Mw, 80,000–100,000 and ~700,000), PLGA (LA:GA, 85:15 and 50:50; Mw, 66,000–107,000 and 30,000–60,000, respectively), and PVA (Mw, ~22,000) were purchased from Polyscience Inc. (Warrington, PA, USA), Sigma-Aldrich (St. Louis, MO, USA), and Kanto Chemical Co. Inc. (Tokyo, Japan), respectively. BV was a gift from Sato Pharmaceutical Co., Ltd. (Tokyo). Vybrant™ DiO (3,3'-Dioctadecyloxacarbocyanine perchlorate) cell-labeling solution was obtained from Thermo Fisher Scientific Inc. (Waltham, MA, USA), and Rinderon®-V ointment 0.12% was from Shionogi & Co., Ltd (Osaka, Japan). Other chemicals and reagents were of special or HPLC grade, were obtained commercially, and were used without further purification.

Frozen ears of male and female pigs (LWD, 6-12 months) were purchased from ZEN-NOH Central Institute for Food and Livestock (Tsukuba, Japan). The porcine ears were stored at -80°C until the skin permeation of BV was measured from the nanosheet formulations.

Male hairless rats (WBN/Ila-Ht, weighing 200–250 g), obtained from the Life Science Research Center, Josai University (Sakado, Saitama, Japan) or Ishikawa Experimental Animal Laboratories (Fukaya, Saitama, Japan), were used to evaluate the influence of PLA nanosheets on transepidermal water loss (TEWL). All animal care procedures and experimental protocols were reviewed and approved by the Institutional Animal Care and Use Committee of Josai University.

Three healthy male subjects aged 22–27 years old participated in human studies, in which the adhesiveness to skin and moisture permeability of PLA nanosheets were assessed. The subjects agreed to participate after the purpose and procedures involved in the studies were explained. All

experimental protocols were reviewed and approved by the Human Medical Research Ethical Review Committee of Josai University.

*2.2. Preparation of nanosheet formulations*

Nanosheets were fabricated through a spin-coating-assisted layer-by-layer method using a water-soluble sacrificial membrane (Okamura et al., 2009; Fujie et al., 2007), as shown in Fig. 1. In order to make a sacrificial layer, a 0.5 mL aliquot of 1.0 % PVA in ultra-purified water was dropped onto a silicon oxide ($SiO_2$) substrate (SIO wafer, 200 nm thick of $SiO_2$, SUMCO Co., Tokyo), which was rotated at 4,000 rpm for 20 s by a spin-coater (MS-B100, Mikasa Co. Ltd., Tokyo) and then dried on a hotplate at 50°C for 60 s. The sacrificial layer was spin-coated with 0.5 mL of 0.1–6.0% PLA or PLGA in dichloromethane at 4,000 rpm for 20 s, followed by drying at 50°C for 60 s, resulting in a bilayered film on the $SiO_2$ substrate. When the nanosheet formulations containing BV or DiO were prepared, each chemical was dissolved in the PLA or PLGA solution at 0.1–1.0% or 20 μM concentrations. The PLA or PLGA layer was spontaneously released from the substrate by immersion in water, scooped up with a Teflon mesh (PFA, SEMITEC Co., Osaka), and dried at 50°C for 2 h.

Fig. 1.

*2.3. Morphology of nanosheet formulations*

The macroscopic morphology of the PLA nanosheet formulation containing BV was captured by a digital camera (PEN Lite E-PL6, Olympus Co., Tokyo; M. ZUIKO DIGITAL 14-42 mm F3.5-5.6 II R, Olympus) immediately after floating on the purified water or immediately after application on moistened skin.

The nanosheet surface was observed using a field emission scanning electron microscope (FE-SEM S-4800, Hitachi High-Technologies Co., Tokyo). The nanosheet formulations floating on purified water were scooped with an aluminum oxide membrane (Anodisc®, GH Healthcare UK Ltd., Little Chalfont, UK) and dried in a desiccator at room temperature overnight. The formulations stuck to the membrane were fixed on a stage, and gold was sputtered with a desk-top quick coater (SC-701, Sanyu Electron Co. Ltd., Tokyo) before observation.

The ultraviolet visible light (UV-Vis) absorption spectrum of the nanosheet was measured using a UV spectrophotometer UV-1800 (Shimadzu, Kyoto, Japan).

*2.4. BV content in nanosheet formulations*

BV in the PLA and PLGA nanosheet formulations was extracted with acetonitrile. A nanosheet formulation (20 x 20 mm), which was preweighed together with the Teflon mesh, was soaked in 1.0 mL of acetonitrile and shaken for 30 min. The extract was mixed with an equal volume of acetonitrile containing an internal standard (n-butyl 4-hydroxybenzoate) and the mixture was centrifuged at 21,500 × *g* and 4°C for 5 min. The amount of BV in the supernatant was assayed by high performance liquid chromatography (HPLC). The weight of the formulation was quantified by the difference in the Teflon mesh weight before and after extraction, and the BV content per weight of formulation and per application area was calculated.

*2.5. Adhesiveness of nanosheet formulations*

The adhesive strength of various nanosheet formulations was measured with a microscratch tester for thin films (JISR-3255, Rhesca Co., Tokyo), as described previously (Okamura et al., 2009; Baba et al., 1999). A nanosheet formulation was floated on purified water, scooped with a $SiO_2$ substrate, and then dried in a desiccator at room temperature overnight. The surface of the formulation was scratched using a diamond stylus with a curved radius of 25 µm under optimal conditions; vertical loading rate of 0.17 mN/s, scratch width of 100 µm, and scratch rate of 10 µm/s. When the signal of frictional vibration changed following detachment of formulation from the substrate, the critical load was regarded as the adhesive strength. The strength value was associated with the thickness measured with a microfigure measuring instrument (Surfcorder ET200, Kosaka Laboratory Ltd., Tokyo).

Adhesiveness to human skin was evaluated in healthy subjects, using a nanosheet formulation containing DiO for visualization. Two pieces (10 x 10 mm each) of formulation were applied adjacently to the skin of the inside part of the forearm after washing with water, one of which was covered with a gauze. The DiO nanosheet formulations were observed intermittently on the skin for 12 h at 501 nm by a macrofluorescence and stereomicroscopic system (Olympus Co., Tokyo), which was equipped with a stereomicroscope (SZX7), a fluorescence light source (U-LH100HG), a camera (DP73), and software (cellSens).

*2.6. Moisture permeability of nanosheet formulations*

The breathability of nanosheet formulations containing BV was quantified by the upright cup method based on JIS K 6404-15. A glass cup was filled with 1.0 mL of purified water, covered with a filter paper affixed to a PLA nanosheet, and placed in a thermostatic chamber maintained at 32°C. At predetermined times, the cup was weighed and the amount of water that had evaporated was calculated. The same test was performed for the filter paper-covered or -uncovered cup.

The influence of nanosheets on TEWL was assessed using a VAPO SCAN (AS-VT100RS, Asch Japan Co. Ltd., Tokyo). Rats were anesthetized using an intraperitoneal injection of a combination anesthetic (0.3 mg/kg of medetomidine, 4.0 mg/kg of midazolam, and 5.0 mg/kg of butorphanol) (Bellini et al., 2014). A PLA nanosheet formulation (20 × 20 mm) was applied on the dorsal skin, and the TEWL on the application site was measured with a Vapo Scan (AS-VT100RS, Asch Japan Co. Ltd., Tokyo) for 8 h. The contralateral site across the midline served as control. PLA nanosheets without BV were applied to the forehead, cheek, forearm, and breast skin of healthy human subjects, and TEWL was measured intermittently for 12 h whilst undergoing activities of daily life.

*2.7. BV release from nanosheet formulations*

BV release from various formulations was investigated using a vertical-type diffusion cell (1.77 $cm^2$ of effective diffusion area), in which the receiver chamber was warmed to 32°C (Hatanaka et al., 2015). A nanosheet formulation was applied to a silicone membrane (75 μm thickness, LINTEC Co., Tokyo) after placing in water, the membrane was set in a diffusion cell and excess water was removed. When the nanosheet without BV was used as a controlled-release membrane, the nanosheet was first applied to a silicon membrane and nanosheet formulation was

piled on it. A fingertip unit (1.90 μg/cm$^2$) of commercial ointment was applied onto a silicone membrane that had previously set in a diffusion cell (Finlay et al., 1989). Immediately after applying the formulation, 6.0 mL of 40% (v/v) ethanol-water solution was added to the receiver chamber to initiate the BV-release experiment. Ethanol was added to the receiver solution to maintain the solubility of hydrophobic BV. The silicon membrane was used to prevent the disintegration of all formulations and to minimize membrane resistance to BV diffusion. The receiver solution was stirred with a stirrer bar on a magnetic stirrer and maintained at 32°C until the end of the experiment. An aliquot (0.5 mL) was withdrawn from the receiver chamber and the same volume of 40% (v/v) ethanol-water solution was added to the chamber. The concentration of BV in the sample was determined by liquid chromatography-tandem mass spectrometry (LC/MS/MS) using triamcinolone acetonide as an internal standard.

*2.8. Determination of BV concentration in skin*

A frozen pig ear was thawed at 32°C. The skin was excised, cleaned with water, shaved carefully, and trimmed of excess fat. The formulation was applied and set in the diffusion cell using the same procedure described for the BV-release experiment, except for the use of pig skin instead of silicone membrane. The receiver chamber was filled with 6 mL of water and maintained at 32°C throughout the experiments. The skin was collected 24 h after the application of formulation, and the surface was cleaned with surgical spirit and cotton to completely remove the formulation. Approximately 0.05 g of skin from the formulation-applied area was excised and weighed. After addition of 0.5 mL of water, the skin was homogenized at 12,000 rpm and 4°C for 5 min using a homogenizer (Polytron PT 1200E, Kinematica AG, Littau-Lucerne, Switzerland).

Subsequently, 1.0 mL of ethyl acetate containing an internal standard (triamcinolone acetonide) was added to the homogenate. The mixture was shaken mechanically for 30 min and centrifuged. The ethyl acetate layer was evaporated to dryness under a nitrogen atmosphere. The residue was reconstructed with 0.1 mL of mobile phase of LC/MS/MS and the concentration of BV was determined.

*2.9. Analysis of BV*

A 20 µL sample was injected into an HPLC system. The system (Shimadzu) consisted of a system controller (SCL-10AVP), pump (LC-10AD), auto-sampler (SIL-10AXL), column oven (CTO-10A), UV detector (SPD-10A), and analysis software (LC Solution). An Inertsil® ODS-3 4.6 × 150 mm (GL Sciences Inc.; Tokyo) column was used, which was maintained at 40°C. The mobile phase was acetonitrile: water (50:50), and the flow rate was adjusted to 1.0 mL/min. BV and internal standard were detected at UV 220 nm.

A 10 µL sample was injected into an LC/MS/MS system. The LC system (Shimadzu) consisted of a system controller (CBM-20A), pump (LC-20AD), auto-sampler (SIL-20ACHT), and column oven (CTO-20A). A Shodex ODP2HP-2B 2.0 × 50 mm column and a Shodex ODP2HPG-2A 2.0 × 10 mm guard column (Showadenko Inc., Tokyo) were used, and both were maintained at 40°C. The mobile phase was acetonitrile: methanol: 10 mM ammonium acetate (25:25:50), and the flow rate was adjusted to 0.2 mL/min. Mass spectrometric detection was performed on a 4000QTRAP mass spectrometer (AB Sciex, Tokyo), equipped with an electrospray ionization source. The mass spectrometer was operated at positive-ion mode and ions were detected in the multiple reaction monitoring mode. The optimized mass transition pairs (m/z) were

477.3→279.2 and 435.2→415.2 for BV and the internal standard (triamcinolone acetonide). Data were acquired and quantified using analysis software (Analyst® version 1.4.3, Shimadzu).

## 3. Results

### *3.1. Characteristics of nanosheet formulations*

Figure 2 shows the morphological characteristics of PLA nanosheet formulations containing BV. The formulation was prepared using 1% BV and 1% PLA (Mw, 80,000–100,000) in dichloromethane. High transparency, flexibility, and adhesiveness of PLA nanosheets were maintained, despite the existence of BV (Fig. 2a and b). A high transparency was confirmed by the UV-Vis absorption spectra, in which an absorbance peak at 240 nm was assigned to BV; absorption was hardly observed between 400 and 700 nm (Fig. 2c). SEM images showed that BV crystals existed on the surface of the PLA nanosheet formulation (Fig. 2d), whereas PLA nanosheets without BV had a flat surface (Fig. 2e). The BV content and thickness of nanosheet formulations consisting of various biocompatible polymers are listed in Table 1. The formulations were prepared using 1% BV and 1% polymer in dichloromethane. The formulation consisting of high-molecular weight PLA possessed high BV content and thickness. The BV content decreased with the increase in GA ratio of polymers, whereas there was minimal change in thickness.

Fig. 2.

Table 1

### *3.2. Adhesiveness of nanosheet formulations*

Figure 3 shows the relationship between the adhesive strength and thickness of nanosheet formulations prepared using 1% BV and 1% polymer in dichloromethane. Nanosheet data, in the absence of BV, and previously reported data, in which PLA (Mw 80,000–100,000) nanosheets were prepared using various concentration of PLA dichloromethane solutions without BV, are also shown (Okamura et al., 2009). The thinner the PLA nanosheet, the stronger the adhesive strength. Although the presence of BV increased the thickness of the nanosheets, the influence on thickness, and hence adhesiveness, was minimal.

A PLA (Mw 80,000–100,000) nanosheet formulation containing DiO was applied to human skin was observed intermittently for 12 h (Fig. 3). The formulation adhered to the skin for 12 h in the presence and absence of a gauze.

Fig. 3.

Fig. 4.

### *3.3. Moisture permeability of nanosheet formulations*

Moisture permeability of nanosheet formulation was assessed *in vitro* and *in vivo* (Fig. 5). The PLA (Mw 80,000–100,000) nanosheet formulation containing BV had no effect on water

evaporation and the TEWL of rat back skin (Fig. 5a and b). The PLA nanosheet did not affect the TEWL of human cheek, forehead, arm, or breast skin (Fig. 5c-f).

Fig. 5.

*3.4. BV release from nanosheet formulations*

The profiles of BV release from nanosheet formulations fabricated under a variety of conditions were compared with those of a commercial ointment (Fig. 6). The nanosheet formulation consisting of high-molecular weight PLA demonstrated high BV releasing properties (Fig. 6a). An increase in the GA ratio of polymer resulted in a decrease in the amount of BV released from the nanosheet formulations (Fig. 6b). Because higher amounts of BV were released from the nanosheet formulation prepared using 1% BV dichloromethane solution compared with a commercial ointment, controlled release of BV was attempted. The amount of BV released decreased with decreasing BV concentration in dichloromethane solutions (Fig. 6c). When a PVA nanosheet without BV was placed on the nanosheet formulation as a controlled-release membrane, BV release was suppressed (Fig. 6d). This suppression intensified when the number of controlled release membranes was increased.

Fig. 6.

### *3.5. BV concentration in skin following the application of nanosheet formulations*

Figure 7 shows the BV concentration in porcine skin 24 h after the application of various formulations. The skin concentration of BV after the application of PLA nanosheet formulations with or without a mono-layered controlled-release membrane were similar to that after the application of commercial ointment. The amount of BV that permeated through the skin was less than the detection limit (approximately 1 ng) for 24 h.

Fig. 7.

## 4. Discussion

The present study was performed to assess the possible use of biocompatible polymeric nanosheets as topical and transdermal devices using BV as a model drug. The nanosheets have high flexibility and adhesiveness due to the high aspect ratio (Okamura et al., 2009; Okamura et al., 2013; Komachi et al., 2017). The application of nanosheets as a dressing following the topical application of drugs, such as tetracycline and silver sulfadiazine, has been reported (Fujie et al., 2010; Ito et al., 2015). If nanosheets can incorporate and release therapeutic levels of drugs, they have potential for the development of a new type of topical and transdermal device, for the precise delivery of drugs to any area of skin.

Whether ultra-thin nanosheets can carry adequate levels of drugs remains a concern. However, when nanosheet formulations were fabricated using 1% BV and 1% polymer dichloromethane

solutions in the present study, the BV contents were about 10–20% (Table 1), which was markedly higher than the 0.12% content of commercial ointment. The amount of drug per unit area of skin was approximately 5–10 μg/cm$^2$. These values were higher than 1.90 μg/cm$^2$, which was calculated based on the fingertip unit concept for steroid therapy (Finlay et al., 1989). In the spin-coating-assisted layer-by-layer self-assembly method, thin film formation is promoted by centrifugal and air shear forces (Ma and Hwang, 1990). Adsorption and rearrangement of adsorbed polymer chains on the surface of the substrate and elimination of weakly bound polymer chains from the substrate occur simultaneously at a high spinning speed for a short period of time (Cho et al., 2001). BV is incorporated into the thin film together with surface adsorption of polymer chains and the excess is crystallized on the film. Since BV is a hydrophobic drug (XLogP3, 3.6) (Cheng et al., 2007), its concentration in the nanosheet formulations increased as the hydrophobicity of polymers, used as building blocks, increased, which was provided by a high-molecular weight and low GA ratio (Table 1). BV crystals were observed on the surface of the PLA nanosheet formulation by SEM (Fig. 2c and d). A part of BV solved in the polymer matrices and the remaining BV crystallized along with the evaporation of solvent. Pores, which may be formed by the evaporation of solvent, were also observed (Fig. 2c). This phenomenon has been reported in percutaneous absorption tape preparations made from pressure-sensitive adhesives (Hatanaka et al., 1991). The high BV content of nanosheet formulations was due to the BV crystals. It was difficult to develop a nanosheet formulation using a higher concentration of BV than PLA. When the nanosheet formulation on the $SiO_2$ substrate was immersed in water, some fragments of film were released due to the insufficient entanglement of polymer chains (data not shown).

Despite the high BV content, the adhesiveness of nanosheet formulations remained high (Fig. 4). The formulations remained on the skin for 12 h and could be removed by washing with soap

and water (data not shown). Although fluorescence declined in the nanosheet formulation that was not covered with gauze, the formulation itself remained on the skin for 12 h. The adhesive strength of nanosheets depends on their thickness (Okamura et al., 2009). The decreased interaction of polymer chains in the ultra-thin film has been reported to decrease the glass transition temperature, resulting in a polymer with high flexibility and adhesiveness (Mattsson et al., 2000). Minimal changes in nanosheet thickness were observed following the incorporating of BV, resulting in the high adhesiveness of nanosheet formulations (Fig. 3). The transparency of nanosheets was also unaffected by BV probably, due to their thinness (Fig. 2a and b). This is favorable for drugs applied to exposed areas of skin, such as the face, where appearance may be important.

Moisture permeability is an important property for topical and transdermal devices, because the increased sweat volume due to occlusion may exacerbate miliaria rubra (Ale et al., 2009). The PLA nanosheet formulation containing BV did not affect water evaporation or TEWL of rat skin, and the PLA nanosheet did not alter the TEWL of human skin (Fig. 5). The TEWL values for anesthetized rats decreased over time, because of dehydration (Fig. 5b). The TEWL value was highest in human forehead skin, as followed by cheek, breast, and arm skin (Fig. 5c-f). Differences in TEWL between application sites may be associated with differences in drug absorption (Machado et al., 2010). The semi-crystalline domains and microscopic apertures in nanosheets are formed by polymer chains (Fujie et al., 2013). Small water molecules can diffuse in the apertures.

The biocompatible polymeric nanosheets not only contain BV, but also release it (Fig. 6). High amounts of BV were released from the nanosheet formulation consisting of hydrophobic polymers, reflecting the high BV content (Table 1, Fig. 6a and b). The high BV release from the nanosheet formulations compared with the commercial ointment requires a controlled-release strategy. The use of a low BV concentration in dichloromethane solutions reduced the BV content

in nanosheet formulations, resulting in low levels of BV release (Fig. 6c). The use of a layered PLA nanosheet as a controlled-release membrane reduced the amount of BV released from the nanosheet formulation, and the effect of a bi-layered nanosheet was superior to that of a mono-layered one (Fig. 6d). The permeability of molecules across PLA nanosheets depends on their thickness and on the molecular size of the permeants (Fujie et al., 2013). The permeability of small and hydrophobic molecules, such as BV (Mw, 476.58), is due to two mechanisms; the semi-crystalline domains and microscopic apertures, which are based on solution-diffusion theory and pore theory, respectively (Hatanaka et al., 1994). Controlled release by a rate-limiting membrane is desirable to prevent overdose following the application of formulations to damaged skin, although the reduced drug content in the formulation is economically favorable.

The BV concentration in porcine skin 24 h after application of nanosheet formulations with and without a controlled-release membrane was similar to that after the application of a commercial ointment (Fig. 7); therefore, sufficient therapeutic effect is obtained with the use of all formulations. These results suggest that the rate-limiting step in the percutaneous absorption of BV is skin permeation, and not BV release from the formulations. However, defects in the epidermal permeability barrier are common in patients treated with steroids (Lee and Lee, 2014). The controlled release of BV from the nanosheet formulations was safe compared with other formulations.

## 5. Conclusion

Biocompatible polymeric nanosheets are promising devices for topical and transdermal drug delivery. They can incorporate and release drugs at therapeutic levels, and the content and amount

released can be controlled by polymers, drug concentrations, and the addition of a controlled-release membrane. Moreover, their high adhesiveness and transparency are retained, even though some drug is incorporated. In addition to the high adhesiveness, the high moisture permeability enables application to any area of skin for a long period of time. Thus, nanosheets may represent a new type of topical and transdermal device, which precisely deliver drugs to any part of the skin. Because they are the transparent, thin-films, they may have application in the cosmetic industry. Further studies are needed to expand the range of usable bioactive compounds. Further development of nanosheet formulations, such as spray formulations, is needed to improve the usability of formulations.

## Acknowledgements

The authors wish to acknowledge technical support from the Technical Service Coordination Office, Tokai University for SEM observations. We gratefully thank Dr. Shinji Takeoka (School of Advanced Science and Engineering, Waseda University) for measuring adhesive strength with a microscratch tester. We would like to thank Editage (www.editage.jp) for English language editing.

## References

Ale, I., Lachapelle, J.M., Maibach, H.I., 2009. Skin tolerability associated with transdermal drug delivery systems: an overview. Adv. Ther. 26, 920–935. https://doi.org/10.1007/s12325-009-0075-9.

Baba, S., Midorikawa, T., Nakano, T., 1999. Unambiguous detection of the adhesive failure of metal films in the microscratch test by waveform analysis of the friction signal. Appl. Surf. Sci. 144–145, 344–349. https://doi.org/10.1016/S0169-4332(98)00824-1.

Bellini, L., Banzato, T., Contiero, B., Zotti, A., 2014. Evaluation of three medetomidine-based protocols for chemical restraint and sedation for non-painful procedures in companion rats (Rattus norvegicus). Vet. J. 200, 456–458. https://doi.org/10.1016/j.tvjl.2014.03.024.

Cevc, G., Blume, G., Schätzleina, A., Gebauer, D., Paul, A., 1996. The skin: a pathway for systemic treatment with patches and lipid-based agent carriers. Adv. Drug Deliv. Rev. 18, 349–378. https://doi.org/10.1016/0169-409X(95)00091-K.

Chang, R.K., Raw, A., Lionberger, R., Yu, L., 2013. Generic development of topical dermatologic products: formulation development, process development, and testing of topical dermatologic products. AAPS J. 15, 41–52. https://doi.org/10.1208/s12248-012-9411-0.

Cheng, T., Zhao, Y., Li, X., Lin, F., Xu, Y., Zhang, X., Li, Y., Wang, R., Lai, L., 2007. Computation of octanol-water partition coefficients by guiding an additive model with knowledge. J. Chem. Inf. Model. 47, 2140–2148. https://doi.org/10.1021/ci700257y.

Cheng, W., Campolongo, M. J., Tan, S. J., Luo, D., 2009. Freestanding ultrathin nano-membranes via self-assembly. Nano Today 4, 482–493. https://doi.org/10.1016/j.nantod.2009.10.005.

Cheng, Y., Xu, Z., Ma, M., Xu, T., 2008. Dendrimers as drug carriers: applications in different routes of drug administration. J. Pharm. Sci. 97, 123–143. https://doi.org/10.1002/jps.21079.

Cho, J., Char, K., Hong, J. D., Lee, K. B., 2001. Fabrication of Highly Ordered Multilayer Films Using a Spin Self-Assembly Method. Adv. Mater. 13, 1076–1078. https://doi.org/10.1002/1521-4095(200107)13:14<1076::AID-ADMA1076>3.0.CO;2-M.

Couvreur, P., Tulkens, P., Roland, M., Trouet, A., Speiser, P., 1977. Nanocapsules: a new type of lysosomotropic carrier. FEBS Lett. 84, 323–326. https://doi.org/10.1016/0014-5793(77)80717-5.

Dalwadi, C., Patel, G., 2015. Application of nanohydrogels in drug delivery systems: recent patents review. Recent Pat. Nanotechnol. 9, 17–25. https://doi.org/10.2174/1872210509666150101151521.

Drugs.com, 2018. Betamethasone Valerate topical. http://www.drugs.com/monograph/betamethasone-valerate-topical.html (accessed 8 May 2018).

Farokhzad, O.C., Langer, R., 2009. Impact of nanotechnology on drug delivery. ACS Nano 3, 16–20. https://doi.org/10.1021/nn900002m.

Finlay, A. Y., Edwards, P. H., Harding, K. G., 1989. “Fingertip unit” in dermatology. Lancet 2, 155. https://doi.org/10.1016/S0140-6736(89)90204-3.

Fujie, T., Okamura, Y., Takeoka, S., 2007. Ubiquitous Transference of a Free-Standing Polysaccharide Nanosheet with the Development of a Nano-Adhesive Plaster. Adv. Mater. 19, 3549-3553. https://doi.org/10.1002/adma.200700661.

Fujie, T., Saito, A., Kinoshita, M., Miyazaki, H., Ohtsubo, S., Saitoh, D., Takeoka, S., 2010. Dual therapeutic action of antibiotic-loaded nanosheets for the treatment of gastrointestinal tissue defects. Biomaterials. 31, 6269–6278. https://doi.org/10.1016/j.biomaterials.2010.04.051.

Fujie, T., Kawamoto, Y., Haniuda, H., Saito, A., Kabata, K., Honda, Y., Ohmori, E., Asahi, T., Takeoka, S., 2013. Selective Molecular Permeability Induced by Glass Transition Dynamics of Semicrystalline Polymer Ultrathin Films. Macromolecules 46, 395–402. https://doi.org/10.1021/ma302081e.

Goenka, S., Sant, V., Sant, S., 2014. Graphene-based nanomaterials for drug delivery and tissue engineering. J. Control. Release 173, 75–88. https://doi.org/10.1016/j.jconrel.2013.10.017.

Gregoriadis, G., 1978. Liposomes in therapeutic and preventive medicine: the development of the drug-carrier concept. Ann. N. Y. Acad. Sci. 308, 343–370. https://doi.org/10.1111/j.1749-6632.1978.tb22034.x.

Hatanaka, T., Oguchi, M., Sugibayashi, K., Morimoto, Y., 1991. Influence of isosorbide dinitrate concentration on its skin permeability from adhesive matrix devices. Chem. Pharm. Bull. 39, 1802–1805. https://doi.org/10.1248/cpb.39.1802.

Hatanaka, T., Manabe, E., Sugibayashi, K., Morimoto, Y., 1994. An application of the hydrodynamic pore theory to percutaneous absorption of drugs. Pharm. Res. 11, 654–658. https://doi.org/10.1023/A:1018911926190.

Hatanaka, T., Yoshida, S., Kadhum, W.R., Todo, H., Sugibayashi, K., 2015. *In silico* estimation of skin concentration following the dermal exposure to chemicals. Pharm. Res. 32, 3965–3974. https://doi.org/10.1007/s11095-015-1756-5.

Hu, X., Liu, S., Zhou, G., Huang, Y., Xie, Z., Jing, X., 2014. Electrospinning of polymeric nanofibers for drug delivery applications. J. Control. Release 185, 12–21. https://doi.org/10.1016/j.jconrel.2014.04.018.

Ito, K., Saito, A., Fujie, T., Nishiwaki, K., Miyazaki, H., Kinoshita, M., Saitoh, D., Ohtsubo, S., Takeoka. S., 2015. Sustainable antimicrobial effect of silver sulfadiazine-loaded nanosheets on infection in a mouse model of partial-thickness burn injury. Acta Biomater. 24, 87–95. https://doi.org/10.1016/j.actbio.2015.05.035.

Kado, Y., Mitsuishi, M., Miyashita, T., 2005. Fabrication of three-dimensional nanostructures using reactive polymer nanosheets. Adv. Mater. 17, 1857–1861. https://doi.org/10.1002/adma.200500884.

Komachi, T., Sumiyoshi, H., Inagaki, Y., Takeoka, S., Nagase, Y., Okamura, Y., 2017. Adhesive and robust multilayered poly(lactic acid) nanosheets for hemostatic dressing in liver injury model. J. Biomed. Mater. Res. B Appl. Biomater. 105, 1747–1757. https://doi.org/10.1002/jbm.b.33714.

Lee, H.J., Lee, S.H., 2014. Epidermal permeability barrier defects and barrier repair therapy in atopic dermatitis. Allergy Asthma Immunol. Res. 6, 276–287. https://doi.org/10.4168/aair.2014.6.4.276.

Liao, C., Li, Y., Tjong, S.C., 2018. Graphene Nanomaterials: Synthesis, Biocompatibility, and Cytotoxicity. Int. J. Mol. Sci. 19, pii: E3564. https://doi.org/10.3390/ijms19113564.

Liu, G., Jin, W., Xu, N., 2016. Two-dimensional-material membranes: A new family of high-performance separation membranes. Angew. Chem. Int. Ed. Engl. 55, 13384–13397. https://doi.org/10.1002/anie.201600438.

Ma, F., Hwang, J. H., 1990. The effect of air shear on the flow of a thin liquid film over a rough rotating disk. J. Appl. Phys. 68, 1265. https://doi.org/10.1063/1.346727.

Machado, M., Salgado, T.M., Hadgraft, J., Lane, M.E., 2010. The relationship between transepidermal water loss and skin permeability. Int. J. Pharm. 384, 73–77. https://doi.org/10.1016/j.ijpharm.2009.09.044.

Mattsson, J., Forrest, J.A., Borjesson, L., 2000. Quantifying glass transition behavior in ultrathin free-standing polymer films. Phys. Rev. E. 62, 5187–5200. https://doi.org/10.1103/PhysRevE.62.5187.

Okamura, Y., Kabata, K., Kinoshita, M., Saitoh, D., Takeoka, S., 2009. Free-standing biodegradable poly(lactic acid) nanosheet for sealing operations in surgery. Adv. Mater. 21, 4388–4392. https://doi.org/10.1002/adma.200901035.

Okamura, Y., Kabata, K., Kinoshita, M., Miyazaki, H., Saito, A., Fujie, T., Ohtsubo, S., Saitoh, D., Takeoka, S., 2013. Fragmentation of poly(lactic acid) nanosheets and patchwork treatment for burn wounds. Adv. Mater. 25, 545–551. https://doi.org/10.1002/adma.201202851.

Osada, M., Sasaki, T., 2012. Two-dimensional dielectric nanosheets: novel nanoelectronics from nanocrystal building blocks. Adv. Mater. 24, 210–228. https://doi.org/10.1002/adma.201103241.

Sarker, D.K., 2005. Engineering of nanoemulsions for drug delivery. Curr. Drug Deliv. 2, 297–310. https://doi.org/10.2174/156720105774370267.

Sugibayashi, K., 2017. Skin Permeation and Disposition of Therapeutic and Cosmeceutical Compounds. Springer Japan, Tokyo.

Tang, W., Bhushan, B., Ge, S., 2010. Friction, adhesion and durability and influence of humidity on adhesion and surface charging of skin and various skin creams using atomic force microscopy. J. Microsc. 239, 99–116. https://doi.org/10.1111/j.1365-2818.2009.03362.x.

Tanner, T., Marks, R., 2008. Delivering drugs by the transdermal route: review and comment. Skin Res. Technol. 14, 249–260. https://doi.org/10.1111/j.1600-0846.2008.00316.x.

Yataba, I., Otsuka, N., Matsushita, I., Matsumoto, H., Hoshino, Y., 2016. The Long-Term Safety of S-Flurbiprofen Plaster for Osteoarthritis Patients: An Open-Label, 52-Week Study. Clin. Drug Invest. 36, 673–682. https://doi.org/10.1007/s40261-016-0412-0.

**Table 1**

BV content and thickness of nanosheet formulations consisting of various biocompatible polymers[a].

| Polymer (LA:GA, Mw) [b] | BV content (μg/mg) [c] | Thickness (nm)[c] |
|---|---|---|
| **PLA (100:0, 80,000–100,000)** | 164.9 ± 17.9 | 99.8 ± 2.9 |
| **PLA (100:0, ~700,000)** | 218.0 ± 15.9 | 182.9 ± 14.2 |
| **PLGA (85:15, 66,000–107,000)** | 148.0 ± 13.5 | 108.3 ± 9.0 |
| **PLGA (50:50, 30,000–60,000)** | 103.8 ± 8.7 | 84.8 ± 7.4 |

[a]The formulations were prepared using 1% BV and 1% polymer in dichloromethane. [b]LA:GA is lactic acid/glycolic acid molecular ratio, and Mw is molecular weight. [c]Each data represents the mean ± standard deviation (S.D.) of four samples.

**Figure captions**

**Fig. 1.** Schematic for the preparation of poly (L-lactic acid) (PLA) nanosheet formulations by a spin-coating assisted layer-by-layer method using a sacrificial membrane. Poly (lactic-co-glycolic) acid (PLGA) nanosheet formulations were fabricated in the same manner using PLGA in substitution of PLA. When betamethasone valerate (BV) was incorporated in the formulations, BV was added to dichloromethane solutions.

**Fig. 2.** Morphological characteristics of PLA nanosheet formulations containing BV. **a)** Macroscopic image of a PLA nanosheet formulation floating in water. **b)** Macroscopic image of a PLA nanosheet formulation applied to the forearm skin of a healthy volunteer. **c)** Ultraviolet visible light absorption spectra of PLA nanosheets with and without BV. **d)** SEM image of a PLA nanosheet formulation. **e)** SEM image of a PLA nanosheet not containing BV. Nanosheets are indicated by arrows in **a)** and a dotted line in **b)**.

**Fig. 3.** Relationship between the adhesive strength and thickness of nanosheet formulations prepared using 1% BV and 1% polymer in dichloromethane. Open circles denote previously reported data [13]. The arrows indicate the change associated with BV. Each data point represents the mean ± S.D. of four samples.

**Fig. 4.** Adhesiveness of nanosheet formulations containing DiO to the skin of healthy human subjects. Observations were made intermittently for 12 h. **a)** With gauze covering. **b)** Without gauze covering.

**Fig. 5.** Moisture permeability of PLA nanosheet formulation. **a)** Water evaporation. **b)** TEWL of rat back skin. **c)** TEWL of human cheek skin. **d)** TEWL of human forehead skin. **e)** TEWL of human arm skin. **f)** TEWL of human breast skin. The PLA (Mw 80,000–100,000) nanosheet

formulations with BV (1% solution) were used for **a** and **b**, and those without BV were used for **c** and **f**. Each data represents the mean ± S.D. of three samples in **a** and **b**, and the raw data from one sample in **c–f**.

**Fig. 6.** Influence of preparation conditions on the BV-releasing profiles of nanosheet formulations. **a)** Molecular weight of PLA. **b)** LA:GA ratio of polymer. **c)** BV concentration in dichloromethane. **d)** PLA nanosheet as a controlled-release membrane. The nanosheet formulations were fabricated using 1% BV dichloromethane solution for **a**, **b**, and **d**. Each data point represents the mean ± S.D. of four samples.

**Fig. 7.** Skin concentration of BV 24 h after the application of a commercial ointment, PLA nanosheet formulation, and a mono-layered controlled-release membrane. The PLA (Mw 80,000–100,000) nanosheet formulations were fabricated using 1% BV dichloromethane solution. Each data point represents the mean ± S.D. of four samples.

1 Fig.1.

2

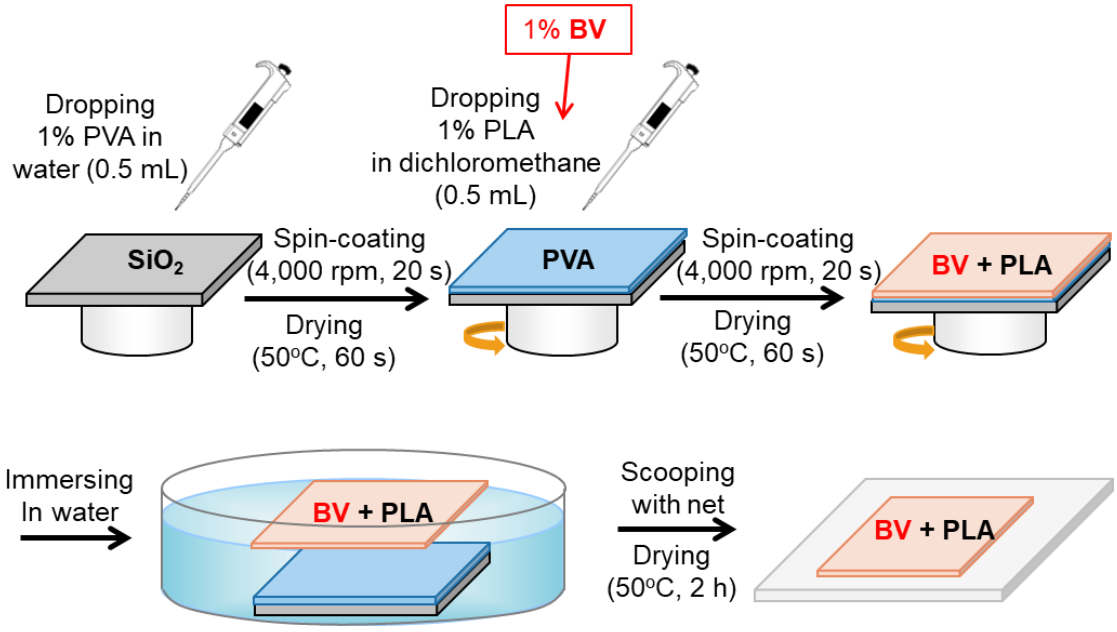
1% BV
Dropping
1% PVA in
water (0.5 mL)
Dropping
1% PLA
in dichloromethane
(0.5 mL)
SiO2
Spin-coating
(4,000 rpm, 20 s)
Drying
(50°C, 60 s)
PVA
Spin-coating
(4,000 rpm, 20 s)
Drying
(50°C, 60 s)
BV + PLA
Immersing
In water
BV + PLA
Scooping
with net
Drying
(50°C, 2 h)
BV + PLA

1 Fig. 2.

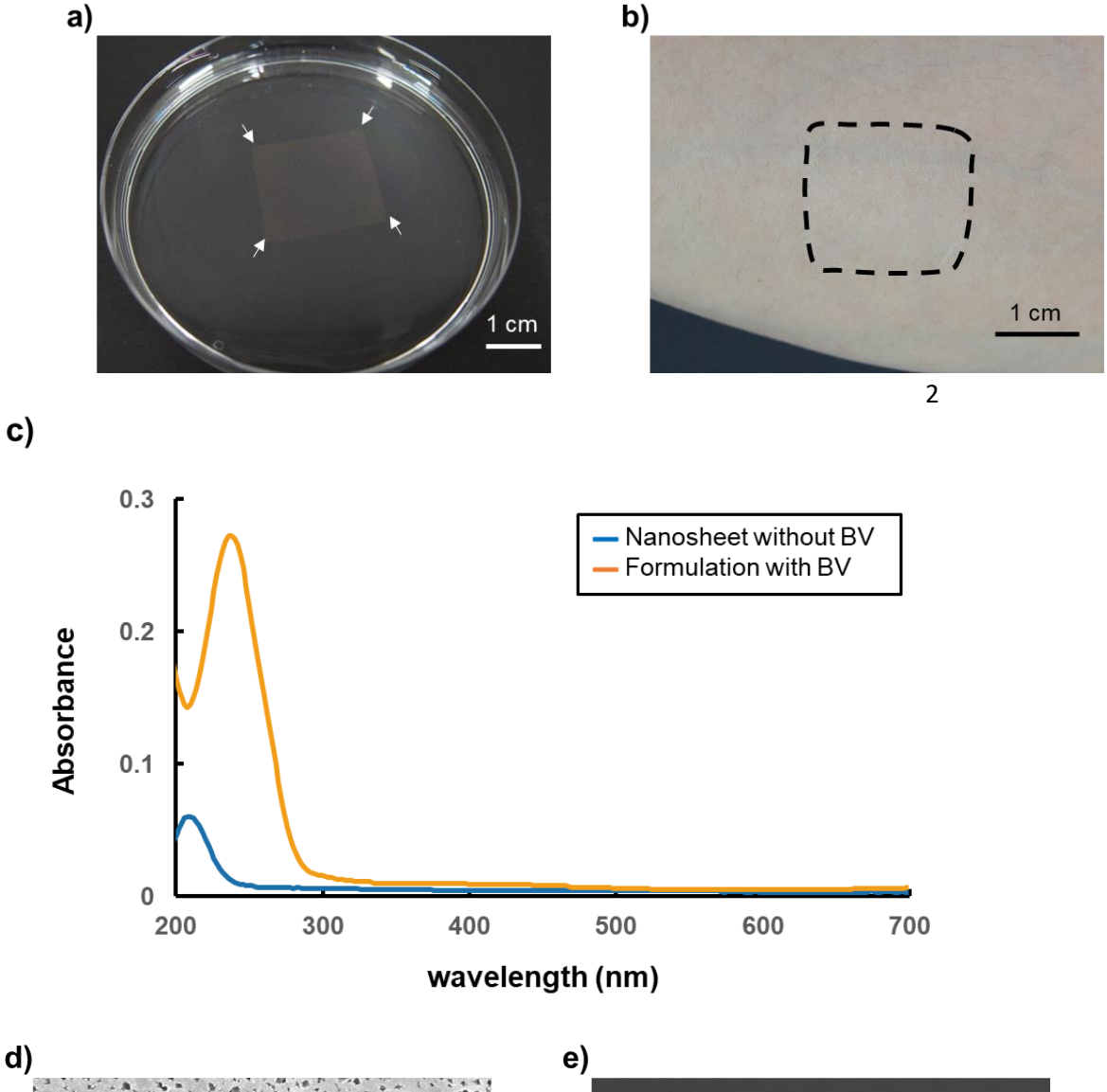
a)
1 cm
b)
1 cm
c)
0.3
0.2
0.1
0
Absorbance
200
300
400
500
600
700
wavelength (nm)
Nanosheet without BV
Formulation with BV
d)
1 µm
e)
0.5 µm

2

1 Fig. 3.

2

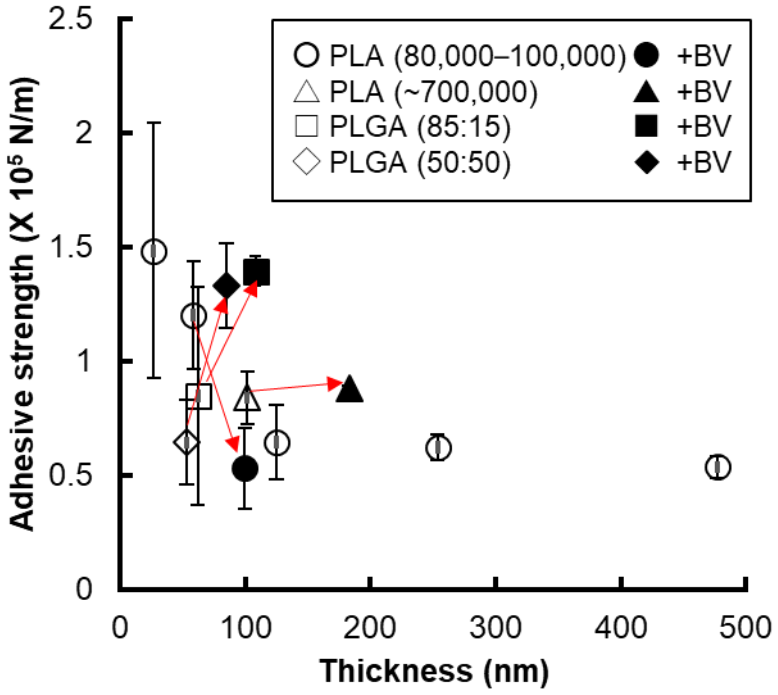
Adhesive strength (X 10⁵ N/m)
2.5
2
1.5
1
0.5
0
0
100
200
300
400
500
Thickness (nm)
PLA (80,000–100,000)
+BV
PLA (~700,000)
+BV
PLGA (85:15)
+BV
PLGA (50:50)
+BV

1 Fig. 4.

2

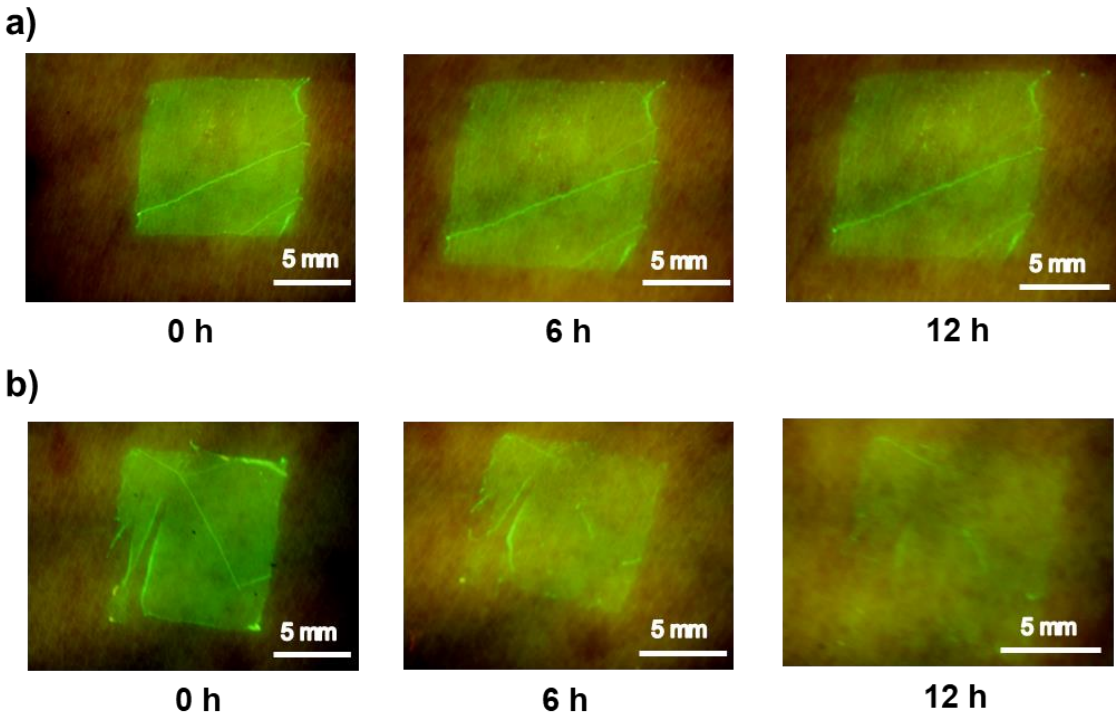

1 Fig. 5.

2

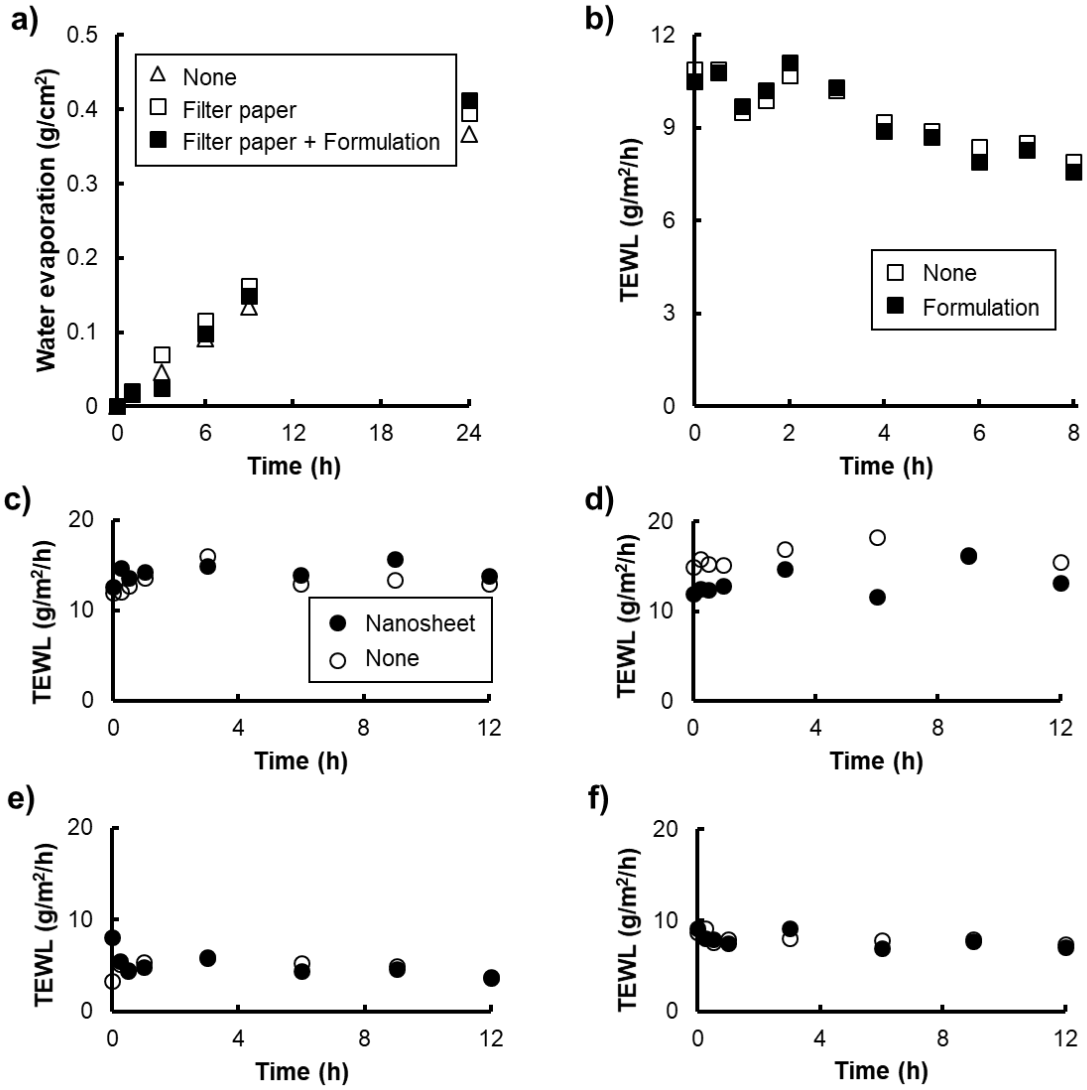
a)
Water evaporation (g/cm²)
0.5
0.4
0.3
0.2
0.1
0
None
Filter paper
Filter paper + Formulation
0
6
12
18
24
Time (h)
b)
TEWL (g/m²/h)
12
9
6
3
0
None
Formulation
0
2
4
6
8
Time (h)
c)
TEWL (g/m²/h)
20
10
0
Nanosheet
None
0
4
8
12
Time (h)
d)
TEWL (g/m²/h)
20
10
0
0
4
8
12
Time (h)
e)
TEWL (g/m²/h)
20
10
0
0
4
8
12
Time (h)
f)
TEWL (g/m²/h)
20
10
0
0
4
8
12
Time (h)

1 Fig. 6.

2

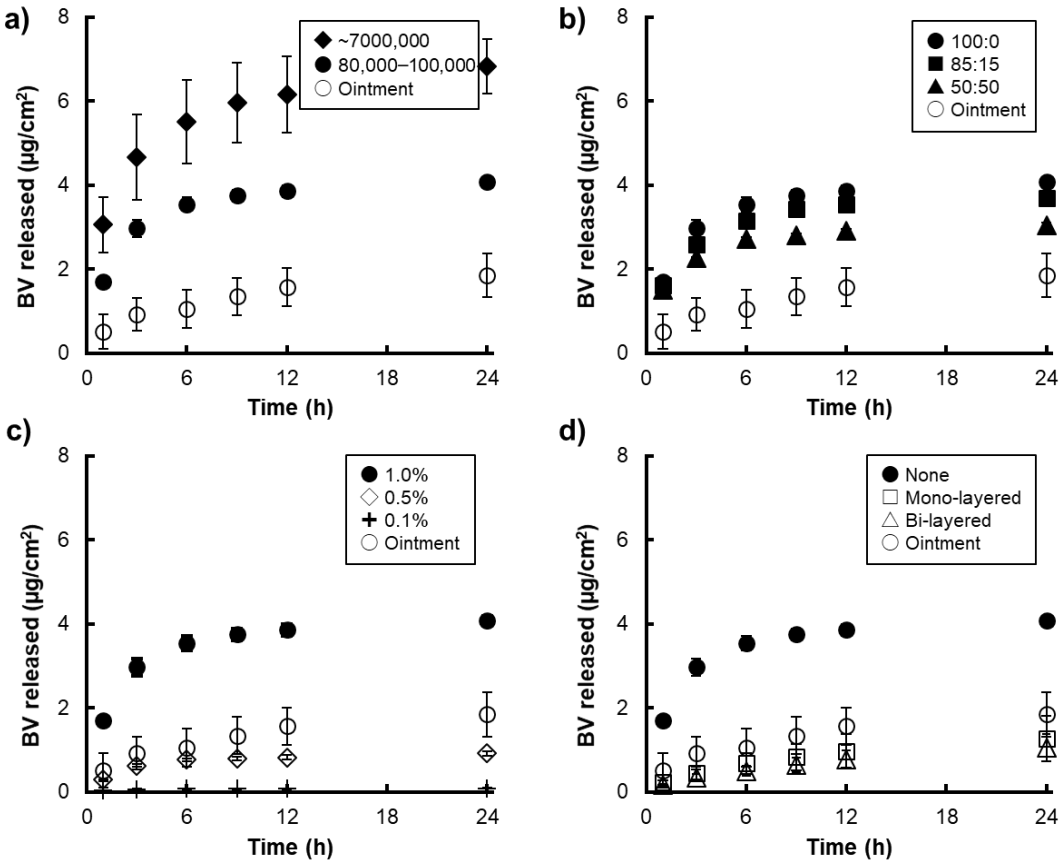
a)
BV released (μg/cm²)
Time (h)
~7000,000
80,000–100,000
Ointment
b)
100:0
85:15
50:50
Ointment
c)
1.0%
0.5%
0.1%
Ointment
d)
None
Mono-layered
Bi-layered
Ointment

1 Fig. 7.

2

3

4

5

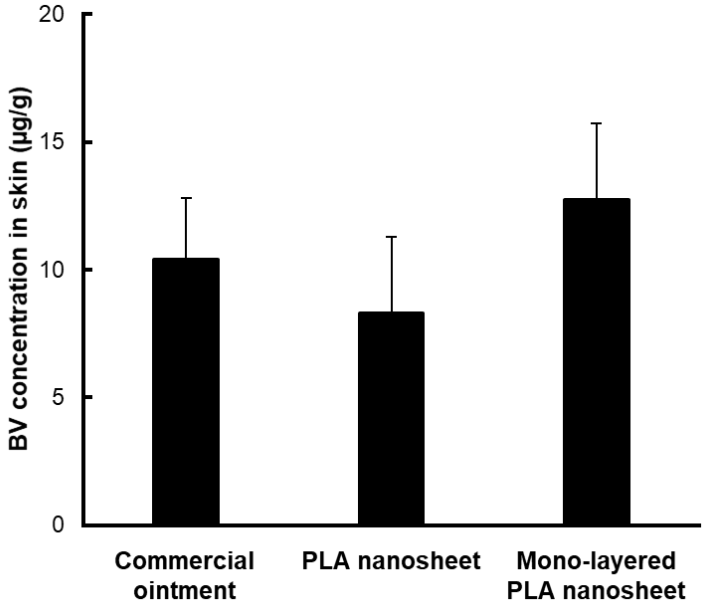
BV concentration in skin (μg/g)
20
15
10
5
0
Commercial ointment
PLA nanosheet
Mono-layered PLA nanosheet

1

2

3

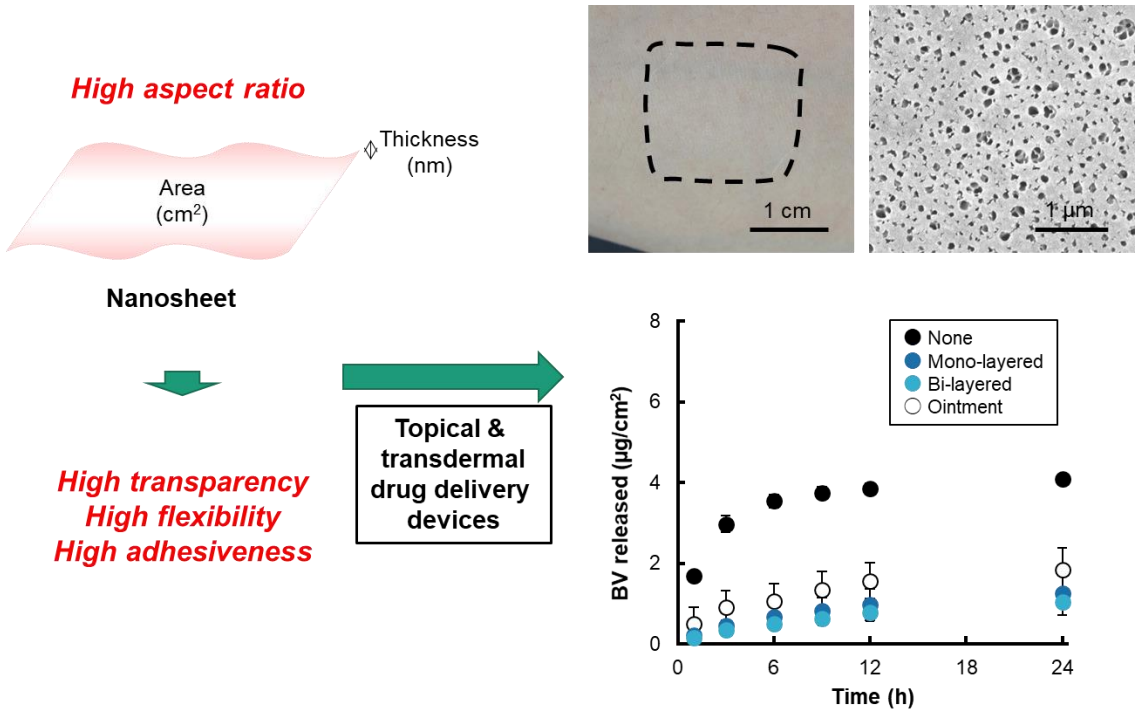
High aspect ratio
Thickness (nm)
Area (cm²)
Nanosheet
High transparency
High flexibility
High adhesiveness
Topical & transdermal drug delivery devices
1 cm
1 μm
None
Mono-layered
Bi-layered
Ointment
BV released (μg/cm²)
Time (h)
0
2
4
6
8
0
6
12
18
24